



HAL
open science

An Integrated Photoacoustic Terahertz Gas Sensor

Mattias Verstuyft, Elias Akiki, Benjamin Walter, Marc Faucher, Mathias Vanwolleghem, Bart Kuyken

► **To cite this version:**

Mattias Verstuyft, Elias Akiki, Benjamin Walter, Marc Faucher, Mathias Vanwolleghem, et al.. An Integrated Photoacoustic Terahertz Gas Sensor. 2019 44th International Conference on Infrared, Millimeter, and Terahertz Waves (IRMMW-THz), Sep 2019, Paris, France. pp.1-2, 10.1109/IRMMW-THz.2019.8873764 . hal-03100252

HAL Id: hal-03100252

<https://hal.science/hal-03100252>

Submitted on 8 Jan 2021

HAL is a multi-disciplinary open access archive for the deposit and dissemination of scientific research documents, whether they are published or not. The documents may come from teaching and research institutions in France or abroad, or from public or private research centers.

L'archive ouverte pluridisciplinaire **HAL**, est destinée au dépôt et à la diffusion de documents scientifiques de niveau recherche, publiés ou non, émanant des établissements d'enseignement et de recherche français ou étrangers, des laboratoires publics ou privés.

An Integrated Photoacoustic Terahertz Gas Sensor

M. Verstuyft¹, E. Akiki², B. Walter³, M. Faucher², M. Vanwolleghem², B. Kuyken¹

¹Photonics Research Group, Department of Information Technology, Ghent University-imec Ghent, Belgium

²IEMN, CNRS UMR 8520, Villeneuve d'Ascq, France

³Vmicro SAS, Villeneuve d'Ascq, France

Abstract—An on-chip gas detector that transduces absorbed terahertz light to a mechanical motion using photoacoustics is proposed. The silicon chip confines light in an optical cavity, wherein an acousto-mechanical cavity is housed. The concentration of a trace gas can be determined from the amplitude of a membrane's motion. The simulations presented predict a minimum detectable limit of 1 ppm of methanol for 1 mW of terahertz power and an integration time of 25 ms.

I. INTRODUCTION

DETECTING terahertz waves at room temperature is difficult for electronic detectors, due its high frequency, on one hand and its low photon energy for optical detectors on the other hand⁴. Specifically for terahertz gas-spectroscopy this is a problem due to low absorption values and hence a low signal-to-noise ratio. In this paper this problem is circumvented by transducing the signal first to sound, and then allowing the sound wave to excite a mechanical motion in a membrane, whose motion forms the final signal (which can be read out using a laser Doppler vibrometer). On one hand this results in a darker background, allowing for better signal-to-noise ratios, on the other hand the signal is enhanced by employing resonators before each transduction of energy: an optical resonator will enhance the light-gas interactions, an acoustic resonator enhances the sound wave and lastly the moving membrane will also be excited resonantly by design.

The optical cavity is comprised of a photonic crystal cavity which confines the light in the central cylindrical hole (mode volume is $1.5 \times 10^4 \mu\text{m}^3$). This hole also forms the acoustic cavity: it is closed on one end by a thin membrane such that it forms a half-open cavity whose fundamental eigenfrequency is at 720 kHz.

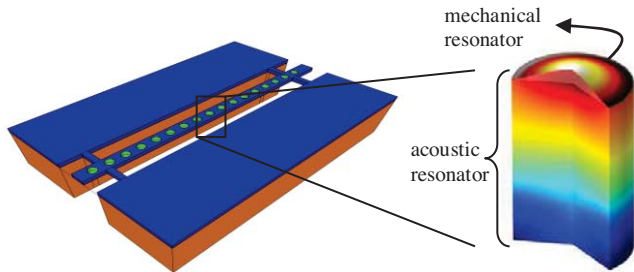


Fig. 1. The three resonators: the central hole of the photonic crystal cavity forms a half-open acoustic cavity, covered by a membrane that functions as a mechanical resonator.

The membrane covering the acoustic resonator is the mechanical resonator that will be excited by the sound waves in the cylinder. It is a low-stress polycrystalline silicon layer of 100nm, whose eigenfrequency matches that of the acoustic resonator.

II. RESULTS

Doing the full simulation of the experiment is computationally very expensive, which is why it is split up into parts. A first simulation is done to determine the amount of light that is absorbed by methanol (as a case study) in the central hole of the photonic crystal cavity (PhCC). This is done using an FDTD simulation: a mode is launched from a waveguide into the PhCCs and a monitor records the absorption in the central hole.

The non-radiative relaxation happens very fast⁵, which is why we assume the conversion into heat to be close to unity. Hence the next simulation consists of a COMSOL Multiphysics setup where a modulated monopole heat source is excited in a half-open cylindrical configuration, whose power reflects the absorption in the FDTD simulation. The purpose here is to determine the conversion efficiency from heat to acoustical power. The losses will be mostly due to both power radiated from the open side, viscous drag effects on the sidewalls of the cylinder and heat conduction through the silicon waveguide. The acoustical quality factor can be found through the formulas¹⁰

$$Q_{rad} = \frac{c_s^2}{2(\pi R f)^2}, \quad Q_{visc} = \sqrt{\frac{\rho \pi R^2 f}{\mu}}$$

with c_s the speed of sound, f the frequency, $R = 30 \mu\text{m}$ the radius of the cylinder and $\mu = 18.1 \mu\text{Pa}\cdot\text{s}$ and $\rho = 1.225 \text{ kg/m}^3$ are the dynamic viscosity and density of air.

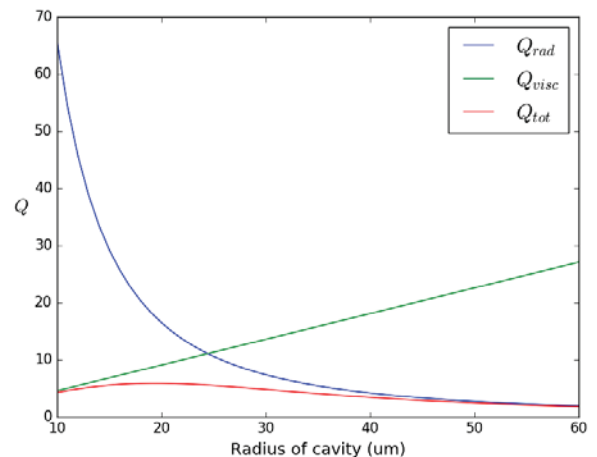


Fig. 2. The total acoustic quality factor is found through $Q_{tot}^{-1} = Q_{rad}^{-1} + Q_{visc}^{-1}$. This illustrates the competing loss mechanisms and the compromise resulting from it.

Unfortunately the radiation loss mechanism is low for narrow cylinders, while the viscous loss is low for wide cylinders. We will hence content ourselves with an acoustic

quality factor below 10, as shown in figure 2. The small mechanical motion of the membrane (the ‘lid’, the motion forming the eventual signal) is neglected in this part. The conversion efficiency from heat to acoustic power increases linearly with the amount of heat created, as expected⁶. It should be noted however that this efficiency is only calculated to understand the physics, as it will again be the same heat source that is used in the final simulation.

Before expanding the previous simulation with a membrane that does move, the mechanical loss mechanisms are discussed.

Anchor losses originate from the fixed constraint on the edges of the membrane. In typical MEMS cantilevers this damping is proportional to the third power of thickness over length⁸. Even though the circular membrane is very different from a cantilever, it provides insight into why the simulated quality factor is high ($Q_{\text{anchor}} = 2 \times 10^6$).

The membrane’s vibration will include local stretching and compression, which will result in temperature variations and hence heat flow. These losses were simulated to be $Q_{\text{TED}} = 4 \times 10^6$, which corresponds to the formula found in literature⁸.

The Akhiezer effect concerns inelastic scattering of phonons. Following the analytic formula⁷ a quality factor of the order of 10^{31} is found, which is why this effect will not be considered in the rest of the model.

Pressure damping is related to the viscous drag that the membrane will experience from oscillating in air rather than in vacuum. This is a significant contributor but will only be included in a later step. The purpose of determining the losses of the mechanical motion is to be able to combine these to one single, mechanical quality factor to be used in the next step, reducing computational power. The anchor and thermoelastic damping are combined into one so-called internal quality factor (Q_{internal}) by making the material’s Young modulus complex³. The pressure damping on the other hand is not included. This will be simulated together with the viscosity effects in the acoustic resonator, as they involve the same physics.

The final simulation is done over a range of modulation frequencies and heat source powers and the membrane’s displacement is recorded. This simulation includes thermoviscous effects, acoustic radiation, heat transfer physics to investigate the heat lost to the silicon waveguides and the mechanical loss mechanisms (through Q_{internal}). Since the displacement (x) is proportional to the square root of the acoustic power (P_{ac}), which in turn is quadratically proportional to the thermal power (P_{th}), the signal ends up being linearly proportional to the concentration of trace gas (c_{gas}).

$$x \sim \sqrt{P_{\text{ac}}} \sim P_{\text{th}} \sim c_{\text{gas}}.$$

Combining this simulation with the FDTD results enables the construction of a function that gives the membrane’s displacement at resonance in function of the trace gas’s concentration, which is plotted in figure 3.

III. CONCLUSIONS

The optical cavity has a mode volume of $1.5 \times 10^4 \mu\text{m}^3$. An FDTD simulation provides the power absorbed by the trace gas in the central hole of the cavity in function of the concentration. The membrane’s losses are split into *internal* losses ($Q_{\text{internal}} = 1.3 \times 10^6$) and *external* losses that are simulated in the final part.

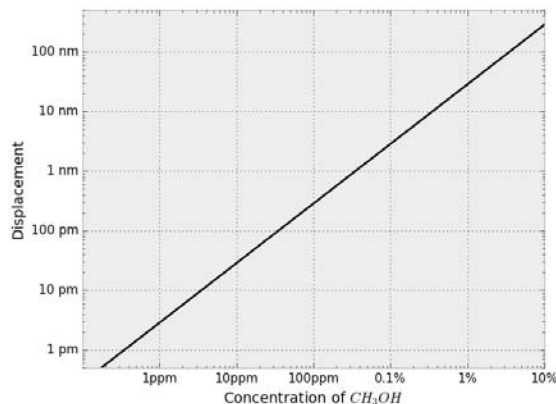


Fig. 3. The simulated displacement of the membrane at resonance for different concentrations of methanol, assuming a source power of 1 mW

The absorbed optical power is used as a thermal monopole source in a further COMSOL simulation using the thermoviscous, solid mechanics and heat transfer modules. The first of these will incorporate both of the acoustic loss mechanisms, as well as the pressure losses of the mechanical resonator. The internal mechanical losses are included in this simulation through the addition of an imaginary part to the membrane’s Young modulus³. The heat transfer module includes the effect of heat lost to the silicon waveguide.

The thermal monopole source is excited at different frequencies and the membrane’s displacement at resonance is plotted in figure 3, in function of the concentration of methanol. Using a commercially available laser Doppler vibrometer⁹ a detection limit of 1 ppm of methanol for a source of 1 mW and an integration time of 25 ms is concluded.

REFERENCES

- [1]. M. Giglio, et al., «Damping Mechanisms of Piezoelectric Quartz Tuning Forks Employed in Photoacoustic Spectroscopy for Trace Gas Sensing», *Physica Status Solidi*, 1800552, 1–7, 2019.
- [2]. M. Gologanu, et al., «Damping effects in MEMS resonators », *CAS International Semiconductor Conference*, 2012.
- [3]. D. Montalvao, R. Claudio, et al., “Experimental measurement of the complex Young’s modulus on a CFRP laminate considering the constant hysteretic damping model”, *Composite Structures*, 97, 91-98, 2013.
- [4]. F. Sizov and A. Rogalski, “THz detectors”, *Progress in Quantum Electronics*, 34, 278–347, 2010.
- [5]. P. Patimisco, et al., “Quartz-enhanced photoacoustic spectroscopy: a review”, *Sensors*, 14, 6165–6206, 2014.
- [6]. M. Daschewski, et al., “Physics of thermo-acoustic sound generation”, *Journal of Applied Physics*, 114, 903, 2013.
- [7]. S. Ghaffari, et al., “Accurate modeling of quality factor behavior of complex silicon MEMS resonators”, *Journal of Microelectromechanical Systems*, 24(2), 276–288, 2015.
- [8]. J. Rodriguez, et al., “Direct Measurements of Anchor Damping in MEMS Resonators”, *IEEE Sensors*, (2), 2–4, 2017.
- [9]. M. Johansmann, et al., “Targeting the Limits of Laser Doppler Vibrometry”, 2005.
- [10]. M.J. Moloney, et al., “Acoustic quality factor and energy losses in cylindrical pipes”, *American Journal of Physics* 69, 311, 1–5, 2001.